International Journal of Cardiology 285 (2019) 32–39

Contents lists available at ScienceDirect

International Journal of Cardiology

journal homepage: www.elsevier.com/locate/ijcard

Electrical remodeling after percutaneous atrial septal defect closure in pediatric and adult patients

Vivian P. Kamphuis [a,b,*,1], Martina Nassif [c,1], Sum-Che Man [d], Cees A. Swenne [d], Jan A. Kors [e], A. Suzanne Vink [c], Arend D.J. ten Harkel [a], Arie C. Maan [d], Barbara J.M. Mulder [b,c], Rob J. de Winter [c], Nico A. Blom [a,f]

[a] Department of Pediatric Cardiology, Leiden University Medical Center, Leiden, the Netherlands
[b] Netherlands Heart Institute, Utrecht, the Netherlands
[c] Department of Cardiology, Academic Medical Center, Amsterdam, the Netherlands
[d] Department of Cardiology, Leiden University Medical Center, Leiden, the Netherlands
[e] Department of Medical Informatics, Erasmus University Medical Center, Rotterdam, the Netherlands
[f] Department of Pediatric Cardiology, Academic Medical Center, Amsterdam, the Netherlands

ARTICLE INFO

Article history:
Received 10 August 2018
Received in revised form 17 November 2018
Accepted 11 February 2019
Available online 23 February 2019

Keywords:
Atrial septal defect
Electrocardiography
Vectorcardiography
Ventricular gradient
QRS-T angle

ABSTRACT

Background: Several studies have reported changes in electrocardiographic variables after atrial septal defect (ASD) closure. However no temporal electro-and vectorcardiographic changes have been described from acute to long-term follow-up at different ages. We aimed to study electrical remodeling after percutaneous ASD closure in pediatric and adult patients.

Methods: ECGs of 69 children and 75 adults (median age 6 [IQR 4–11] years and 45 [IQR 33–54] years, respectively) were retrospectively selected before percutaneous ASD closure and at acute (1–7 days), intermediate (4–14 weeks) and late (6–18 months) follow-up. Apart from electrocardiographic variables, spatial QRS-T angle and ventricular gradient (VG) were derived from mathematically-synthesized vectorcardiograms.

Results: In both pediatric and adult patients, the heart rate decreased immediately post-closure, which persisted to late follow-up. The P-wave amplitude also decreased acutely post-closure, but remained unchanged at later follow-up. The PQ duration shortened immediately in children and at intermediate follow-up in adults. The QRS duration and QTc interval decreased at intermediate-term follow-up in both children and adults. In both groups the spatial QRS-T angle decreased at late follow-up. The VG magnitude increased at intermediate follow-up in children and at late follow-up in adults, after an initial decrease in children.

Conclusion: In both pediatric and adult ASD patients, electrocardiographic changes mainly occurred directly after ASD closure except for shortening of QRS duration and QTc interval, which occurred at later follow-up. Adults also showed late changes in PQ duration. At 6-to-18 month post-closure, the spatial QRS-T angle decreased, reflecting increased electrocardiographic concordance. The initial acute decrease in VG in children, which was followed by a significant increase, may be the effect of action potential duration dynamics directly after percutaneous ASD closure.

1. Introduction

The ostium secundum atrial septal defect (ASD) is one of the most common congenital heart diseases and is defined as an interatrial septum defect at the site of the fossa ovalis, causing a left-to-right shunt [1]. A hemodynamically significant shunt causes volume overload of the right atrium (RA), right ventricle (RV) and the pulmonary circulation, and is, therefore, an indication for ASD closure, to prevent further right-sided deterioration such as volume and/or pressure overload and eventually heart failure [2]. Closing an ASD-based left-to-right shunt initiates both geometrical and electrical RA and RV remodeling [3,4], the extent of which may depend on several factors including the patients' age at closure and closure technique. Percutaneous ASD closure is currently the first choice of treatment in selected cases, due to the minimal invasiveness, and has proven to reduce morbidity and mortality similar to surgical closure [1].

* Corresponding author at: Department of Pediatrics, Division of Pediatric Cardiology, Leiden University Medical Centre, Leiden, the Netherlands.
E-mail addresses: v.p.kamphuis@lumc.nl (V.P. Kamphuis), m.nassif@amc.uva.nl (M. Nassif), s.man@lumc.nl (S.-C. Man), C.A.Swenne@lumc.nl (C.A. Swenne), j.kors@erasmusmc.nl (J.A. Kors), a.s.vink@amc.uva.nl (A.S. Vink), A.D.J.ten_Harkel@lumc.nl (A.D.J. ten Harkel), A.C.Maan@lumc.nl (A.C. Maan), b.j.mulder@amc.uva.nl (B.J.M. Mulder), r.j.dewinter@amc.uva.nl (R.J. de Winter), N.A.Blom@lumc.nl (N.A. Blom).
[1] Both authors contributed equally to this manuscript.

https://doi.org/10.1016/j.ijcard.2019.02.020

The electrocardiogram (ECG) is the standard tool to visualize cardiac electrical activity, and after ASD closure it can show potential complications like atrial arrhythmias [2], as well as the electrical reverse remodeling at several post-procedural time points. The latter gives insight into the long-term process of reverse remodeling, in which a distinction is made between acute and late effects of ASD closure. The standard 12-lead ECG only allows for scalar, one-dimensional, visualization of the electrical currents in the heart. The vectorcardiogram (VCG), however, offers several advantages over the 12-lead ECG. Firstly, the lead vectors of the X-, Y- and Z-lead assume the directions of the main anatomical axes of the body. Furthermore, the sensitivities of these X-, Y- and Z-lead are equal. Lastly, by displaying the instantaneous electrical heart activity (represented as the heart vector) in three-dimensional (3D) space, the phase-relationships between the X-, Y- and Z-leads become apparent [5]. Historically, the VCG was recorded directly with the Frank VCG system; currently, conversion of a 12-lead ECG to a VCG by mathematical transformation (using the inverse Dower or Kors matrix [6]) is the standard. Two vectorcardiographic variables in particular have recently gained interest: the ventricular gradient (VG), which has been shown useful in the detection of RV pressure overload [7], and the spatial QRS-T angle, which has shown prognostic value in the prediction of sudden cardiac death [8].

Several studies have reported changes in ECG variables after ASD closure [3,9–12], however no temporal ECG and VCG changes have been described from acute to long-term follow-up at different ages. Hence, the objective of this study was to assess acute, intermediate and late electrical remodeling in terms of ECG and VCG changes after ASD closure in both children and adults.

2. Materials and methods

2.1. Study design and population

In this multicenter retrospective cohort study, all patients with an ASD who were referred to the Center for Congenital Heart Disease Amsterdam Leiden (CAHAL) for percutaneous ASD closure in a period of 13 months (2016–2017) were screened. The study cohort comprised of pediatric (age 0–17 years) and adult patients (age ≥ 18 years) who had a 12-lead ECG in sinus rhythm maximally 14 weeks before successful ASD closure and at acute (1–7 days) or intermediate (4–14 weeks) follow-up after closure. Additionally, when available in these patients, ECGs that were made late (6–18 months) after closure were also assessed. All the included ECGs were made as part of routine clinical follow-up. Baseline patient characteristics, clinical history and medication were collected from medical records. The Medical Ethics Committee provided a statement of no objection for obtaining and publishing the anonymized data.

2.2. ASD closure

Percutaneous ASD closure was performed conform current guidelines, in which ASD closure is indicated in the presence of hemodynamically significant left-to-right shunting with pulmonary vascular resistance <5 Woods units (Class I, level B) [2]. Patients underwent general anesthesia and an Amplatzer Septal Occluder (Abbott Vascular Inc., Santa Clara, CA, USA) of appropriate size was implanted under transesophageal echocardiographic guidance.

2.3. ECG/VCG processing

All ECGs made in the Leiden University Medical Center, Leiden, The Netherlands, were recorded with ELI 250 and 350 electrocardiographs (Mortara Instrument, Milwaukee, USA) with a sampling rate of 1000 samples per second. The ECGs made in The Academic Medical Center Amsterdam, The Netherlands, were recorded with MAC5500 electrocardiographs (GE Healthcare, Milwaukee, USA) with sampling rates of 250 or 500 samples per second. All ECG and VCG measurements were performed with the Modular ECG Analysis System (MEANS) [13], which has been evaluated extensively, both by its developers and by others [14,15]. For each lead, MEANS performs baseline correction, removes main interference, and computes a representative averaged beat after excluding ectopic beats. MEANS determines global fiducial points in the averaged beats of all 12 leads together, resulting in an overall P-wave onset, P-wave offset, QRS complex onset and offset, and T-wave offset. The following ECG variables were assessed: heart rate, P-wave amplitude in lead II, P-wave duration, PQ duration, QRS duration and the QT interval, corrected with Bazett's formula (QTc).

The X-, Y- and Z leads of the VCGs were synthesized from the ECGs by the Kors transformation matrix [6]. For the directions of the X-, Y- and Z axes and the spatial vector orientation (azimuth, elevation), the American Heart Association VCG standard was followed [16]. From the VCG, the spatial QRS-T angle was computed as the spatial angle between the QRS-and T-integral vectors. Also, the azimuth, elevation and magnitude of the VG (vectorial sum of the QRS and the T integrals) were assessed, as well as its components in the X-, Y- and Z-direction (VG_x, VG_y and VG_z).

2.4. Statistical analysis

Statistical analysis was performed in SPSS v.23 (IBM, Armonk, NY, USA). Quantitative data are presented as median [25th–75th percentile] with minimum and maximum where relevant for continuous variables, and as frequencies (percentages) for categorical variables. Comparisons between ECG- and VCG parameters at different time points (i.e. acute, intermediate and late follow-up) included one ECG/VGG per time interval and were performed using the Wilcoxon signed-rank test. Correlations between ECG/VCG-parameters and patient characteristics were tested using the Spearman correlation. A P-value < 0.05 was considered statistically significant.

3. Results

In total, 168 patients were screened (75 children and 93 adults), of which 144 patients met the inclusion criteria (69 children and 75 adults). Baseline characteristics, stratified into pediatric and adult groups, are shown in Table 1. Not all patients had an ECG at all four time points; absolute numbers are shown in Table 1. Median age of children was 6 years [4–11 years] (range 5 months–17 years) and of adults 45 years [33–54 years] (range 18–79 years). Fourteen adults (19%) had paroxysmal atrial fibrillation.

3.1. ECG changes after ASD closure in children

ECG variables of the pediatric patients at different time intervals are shown in Table 2. In children, heart rate significantly decreased acutely after ASD closure, which became most evident at late follow-up. The P-wave amplitude in lead II showed a significant decrease in the acute period after closure; however, later follow-up showed no significant changes compared to baseline. P-wave duration did not change at post-procedural follow-up. The PQ duration, however, showed a significant decrease from baseline to acute and intermediate follow-up. Compared to the baseline ECG, the QRS duration, as well as the QTc interval, were shorter at intermediate-term follow-up.

Table 1
Baseline patient characteristics of the study cohort.

	Children	Adults
	N = 69	N = 75
Demographics		
Age, y	6 [4–11]	45 [33–54]
Male	26 (38%)	24 (32%)
Body mass index, kg/m^2	16.2 [14.5–18.3]	26 [23–29]
Number of ECGs		
Number of patients with an ECG before closure	69 (100%)	75 (100%)
Number of patients with an ECG at acute follow-up	69 (100%)	74 (99%)
Number of patients with an ECG at intermediate follow-up	32 (46%)	56 (75%)
Number of patients with an ECG at late follow-up	20 (29%)	49 (65%)
Clinical history		
Chromosomal disorder	4 (6%)	0 (0%)
Down syndrome	1 (1%)	0 (0%)
Turner	1 (1%)	0 (0%)
22q11 deletion	1 (1%)	0 (0%)
Smith-Lemli-Opitz syndrome	1 (1%)	0 (0%)
Paroxysmal atrial fibrillation	0 (0%)	14 (19%)
Medication		
Antiarrhythmica (β-blockers)	0 (0%)	5 (6.7%)
QT-prolongating drugs (methylphenidate)	1 (1.4%)	0 (0%)
ASD-related characteristic		
Occluder size	14 [12–18]	22 [17–26]

Data are presented as median [25th–75th percentile] or frequency (%).

Table 2
ECG and VCG results at baseline and post ASD closure.

	Baseline	Acute	*P*-value	Intermediate	*P*-value	Late	*P*-value
	Max −14 w	+1–7 d	Baseline-acute	+4–14 w	Baseline-intermediate	+6–18 m	Baseline-late
ECG results							
Children							
Heart rate, bpm	94 [83–109]	91 [82–102]	0.01	92 [75–102]	0.005	82 [71–92]	0.001
P-wave amplitude in lead II, mV	0.13 [0.11–0.18]	0.11 [0.09–0.15]	<0.001	0.14 [0.12–0.19]	0.51	0.12 [0.08–0.18]	0.55
P-wave duration, ms	94 [92–100]	94 [90–100]	0.24	94 [88–99]	0.08	96 [92–106]	0.24
PQ duration, ms	139 [132–152]	134 [128–148]	0.007	132 [124–149]	<0.001	138 [128–160]	0.52
QRS duration, ms	90 [81–100]	88 [81–97]	0.05	89 [77–98]	<0.001	89 [80–96]	0.06
QTc interval, ms	433 [422–449]	431 [422–447]	0.19	429 [420–440]	0.02	424 [410–448]	0.15
Adults							
Heart rate, bpm	72 [61–81]	67 [59–78]	<0.001	65 [58–76]	0.01	65 [56–74]	<0.001
P-wave amplitude in lead II, mV	0.15 [0.10–0.16]	0.11 [0.08–0.14]	<0.001	0.13 [0.10–0.16]	0.07	0.14 [0.11–0.17]	0.63
P-wave duration, ms	115 [106–125]	114 [104–126]	0.63	112 [102–123]	0.20	113 [104–124]	0.11
PQ duration, ms	163 [150–184]	162 [148–185]	0.62	157 [144–172]	0.01	106 [94–116]	0.009
QRS duration, ms	106 [94–116]	108 [94–118]	0.46	101 [91–112]	0.004	102 [92–109]	<0.001
QTc interval, ms	432 [414–451]	433 [416–449]	0.20	418 [407–441]	0.005	417 [404–435]	<0.001
VCG results							
Children							
Spatial QRST angle, °	52 [30–84]	58 [26–81]	0.05	38 [24–77]	0.44	39 [19–56]	0.002
VG magnitude, mV·ms	63 [48–76]	55 [42–70]	<0.001	78 [64–103]	0.01	83 [68–107]	0.007
VG azimuth, °	−1 [−17–7]	0 [−21–13]	0.69	5 [−6–18]	0.006	1 [−11–18]	0.16
VG elevation, °	39 [34–45]	37 [32–44]	0.71	38 [30–45]	0.16	39 [33–45]	0.96
VG_x, mV·ms	44 [35–58]	37 [28–52]	<0.001	60 [45–74]	0.001	62 [49–78]	0.048
VG_y, mV·ms	39 [29–51]	32 [23–44]	0.001	44 [34–63]	0.23	58 [38–75]	0.02
VG_z, mV·ms	−1 [−15–5]	0 [−15–9]	0.17	4 [−7–17]	0.007	1 [−12−21]	0.03
Adults							
Spatial QRS-T angle, °	42 [21–82]	38 [22–70]	0.79	30 [17–45]	0.39	36 [20–48]	0.001
VG magnitude, mV·ms	66 [45–86]	63 [37–89]	0.32	75 [50–94]	0.08	70 [56–89]	0.001
VG azimuth, °	−12 [−26–0]	−15 [−24 to −3]	0.70	−7 [−17–3]	<0.001	−8 [−24–1]	0.48
VG elevation, °	39 [32–47]	36 [29–41]	<0.001	37 [31–44]	0.07	38 [29–45]	0.65
VG_x, mV·ms	44 [28–60]	50 [22–68]	0.43	55 [38–72]	0.01	52 [38–71]	0.001
VG_y, mV·ms	38 [24–54]	33 [22–45]	<0.001	43 [26–61]	0.23	42 [27–60]	0.002
VG_z, mV·ms	−9 [−20−0]	−12 [−24 to −2]	0.90	−7 [−22−3]	0.006	−8 [−26–1]	0.062

Data are presented as median [25th–75th percentile].
d = days; w = weeks; m = months.

3.2. ECG changes after ASD closure in adults

ECG variables of the adult patients are shown in Table 2 at the different time intervals. In this age group, the heart rate also decreased significantly acutely after intervention. The P-wave amplitude in lead II showed an acute significant decrease, while late effects of ASD closure were not seen. P-wave duration did not change at post-procedural follow-up. However, the PQ duration shortened from baseline to intermediate and late follow-up. Compared to the baseline ECG, QRS duration and the QTc-interval shortened significantly at intermediate-term and late follow-up.

3.3. VCG changes after ASD closure in children

The VCG parameters of pediatric patients are shown in Table 2 for the different time points. The spatial QRS-T angle remained equal at acute and intermediate post-procedural follow-up, but showed a significant decrease at late follow-up. Compared to baseline, VG magnitude significantly decreased acutely after closure, however significantly increased at intermediate and late follow-up. VG azimuth showed a significant change at intermediate follow-up. VG elevation showed no significant changes at follow-up compared to baseline. Fig. 1 shows the spatial median VG changes and the changes projected in each of the three standard planes in the group of pediatric patients. The X-, Y- and Z components of the VG in the pediatric group are shown in Table 2. The VG_x first showed an acute decrease compared to baseline, after which the VG_x increased at intermediate and late follow-up. Similarly, the VG_yalso showed an acute decrease compared to baseline, followed by an increase at late follow-up. The VG_z showed a significant increase at intermediate follow-up and late follow-up.

3.4. VCG changes after ASD closure in adults

The VCG parameters of the adult patients at different time intervals are shown in Table 2. The spatial QRS-T angle remained equal at acute and intermediate post-procedural follow-up, but showed a significant decrease at late follow-up. Compared to baseline, VG magnitude significantly increased at late follow-up. VG azimuth showed a significant change at intermediate follow-up. VG elevation showed an acute decrease but no significant changes compared to baseline at intermediate and late follow-up. Fig. 2 shows the spatial median VG changes and the changes projected in each of the three standard planes in the adult patients. The X-, Y- and Z-coordinates of the VG in the adult group are also shown in Table 2. The VG_x showed an increase at intermediate and late follow-up compared to baseline. The VG_y first showed an acute decrease compared to baseline, after which the VG_y increased again at late follow-up. The VG_z shows a significant increase at intermediate follow-up.

3.5. ECG/VCG parameters in patients with paroxysmal atrial fibrillation

Out of the total study cohort, 14 adults (19%) had paroxysmal atrial fibrillation with sinus rhythm at the time of ECG acquisition. Appendix Table 1 shows the ECG and VCG changes according to presence of paroxysmal atrial fibrillation. In patients with paroxysmal atrial fibrillation, P-wave amplitude decreased acutely, but there were no changes in P-wave duration and PQ duration during follow-up. Furthermore, QRS duration decreased at intermediate follow-up and late follow-up and QTc duration decreased at late follow-up. Regarding VCG changes, the spatial QRS-T angle decreased at intermediate follow-up in patients with paroxysmal atrial

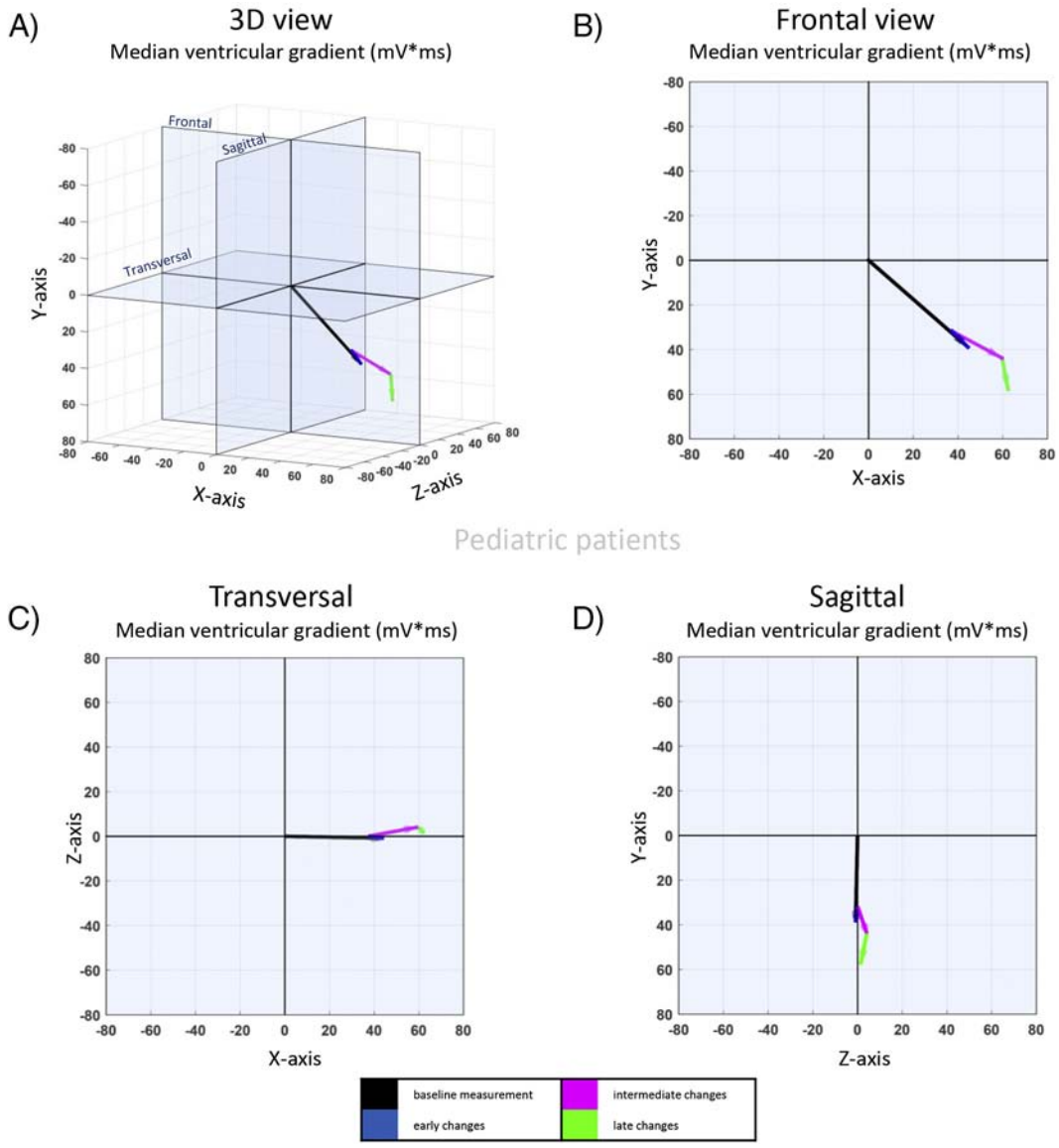

Fig. 1. Spatial changes of the median ventricular gradient in the pediatric patients. A) Three-dimensional (3D) view of the VG changes. B) Frontal view. C) Transversal view. D) Sagittal view. In all images the black line represents the baseline measurement, the blue line represents the early changes, the purple line represents the intermediate changes, and the green line represents the late changes.

fibrillation. Lastly, in these patients, the VG magnitude increased at intermediate follow-up, but did not change at late follow-up.

4. Discussion

In the present study, the acute, intermediate and late electrical remodeling in terms of ECG and VCG changes after percutaneous ASD closure in children and adults was assessed. The main findings of the study are: 1) ASD closure was followed by a decrease in heart rate, P-wave amplitude, PQ duration, QRS duration and QTc interval in both children and adults. Except for the late QRS duration and QTc interval changes, most changes occurred directly after device closure. 2) The spatial QRS-T angle significantly decreased at late follow-up in both children and adults. 3) VG magnitude increased at intermediate follow-up in children and at late follow-up in adults, after an initial decrease in children; the VG direction change was most apparent in the less negative azimuth at intermediate follow-up in both groups; and VG elevation directly decreased in the adult group but did not change during follow-up in the pediatric group.

4.1. Mechanisms of ECG changes after percutaneous ASD closure

Right-sided volume overload due to atrial left-to-right shunting leads to both atrial and ventricular stretch which may cause changes in the 12-lead ECG [4,17] due to mechano-electrical coupling. RA dilatation, for example, may result in increased P-wave amplitude as well as prolonged P-wave duration and increased P-wave dispersion due to delayed atrial conduction, which are all useful markers in the prediction of atrial arrhythmias [3,12]. RV dilatation may result in QRS-duration prolongation, right bundle branch block and crochetage (a notch near the apex of the R-wave in the inferior limb leads [18]). Recently, it has been shown that RV volume overload can cause QTc–interval prolongation in ASD patients [11]. Successful ASD-closure should correct the right-sided volume overload within 24 h, initiating geometric remodeling of the right atrium and ventricle, which continues up to 6–8 weeks following percutaneous ASD closure [4,19]. Indeed, multiple studies reported electrical remodeling after percutaneous ASD closure [3,9–12]. The present study showed a direct decrease in heart rate after ASD closure in both children and adults, with a maintained decrease on the long

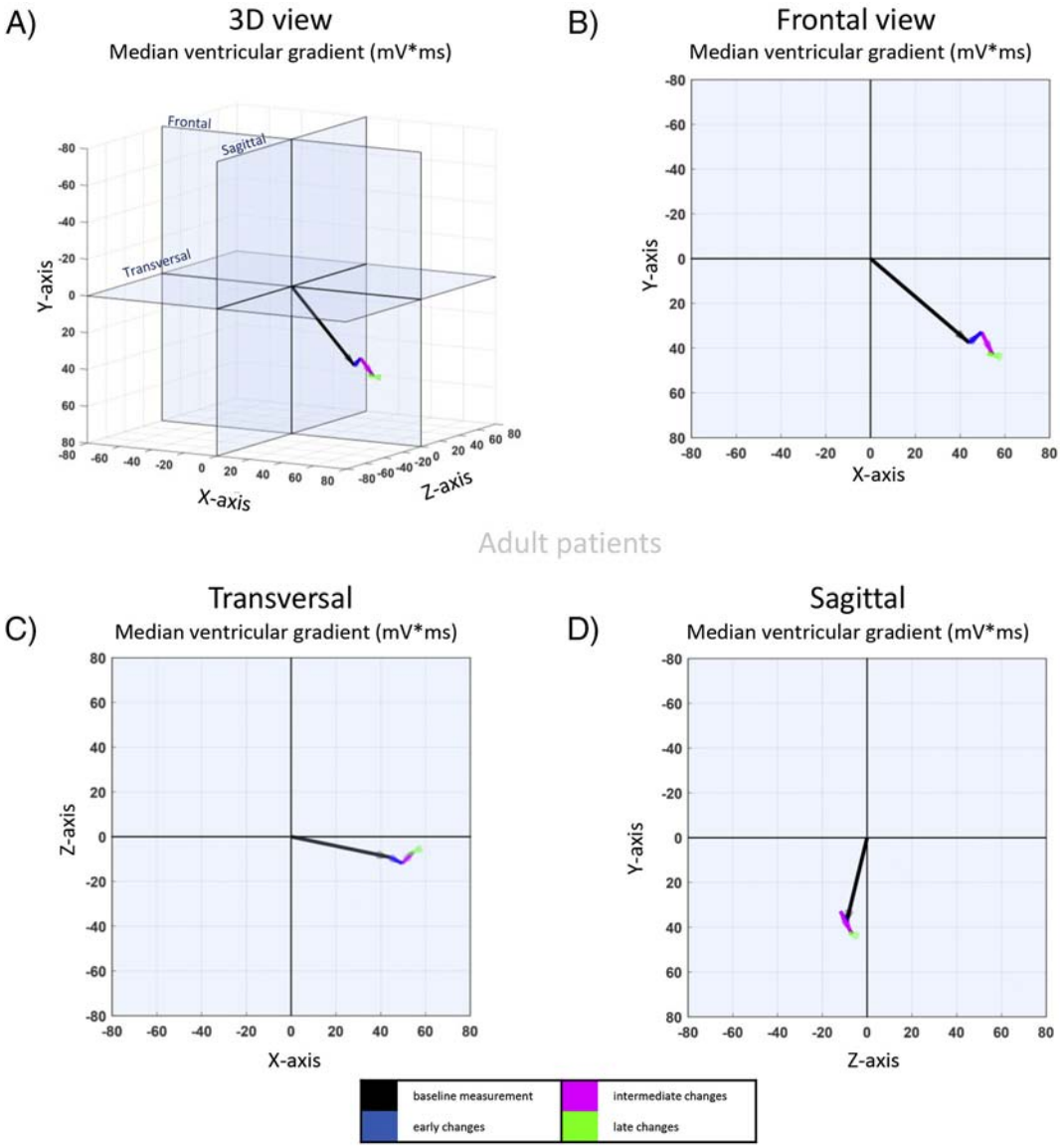

Fig. 2. Spatial changes of the median ventricular gradient in the adult patients. A) Three-dimensional (3D) view of the VG changes. B) Frontal view. C) Transversal view. D) Sagittal view. In all images the black line represents the baseline measurement, the blue line represents the early changes, the purple line represents the intermediate changes, and the green line represents the late changes.

term. We hypothesize that two mechanisms may have contributed to this heart rate decrease: deactivation of the Bainbridge reflex [20] and a decreased stretching of the pacemaking tissue in the sinus node [21]. Heart rate lowering via deactivation of the Bainbridge reflex after ASD can be expected on the basis of deactivation of the stretch receptors at the junction of the vena cava and the right atrium. This will lead to decreased afferent neural traffic via fibers in the vagus nerve that project on the medulla. As a consequence, the reflex-induced inhibition of parasympathetic outflow to the sinus node will be decreased, and the reflex-induced enhancement of sympathetic outflow to the sinus node will be reduced, thus causing a slowing of the heart rate. Furthermore, RA dimensions decrease. Since stretching of the sinus node tissue causes an increased intrinsic pacemaking rate, such decrease in RA size will have also contributed to the observed decrease in heart rate.

In addition, the present study showed an acute decrease in P-wave amplitude in both groups, which is in line with the findings of a previous study done by Grignani et al. [3] They observed an even further decrease in P-wave amplitude at their long-term follow-up of 45 ± 33 months post-closure, suggesting continuation of atrial remodeling over several years. In contrast to other studies [3,10], the present study did not show a decrease in P-wave duration. We did find significant PQ-duration decrease directly after intervention in the pediatric group, and at intermediate follow-up in the adult group. The largest change in PQ duration was seen at late follow-up in the adult group, suggesting that even late after ASD closure atrial remodeling takes place. The latter does not count for patients with paroxysmal atrial fibrillation, in whom PQ duration did not change during follow-up (see Appendix Table 1).

Similar to previous studies [3,10,11], our results support the finding that ventricular electrical remodeling as reflected by QRS duration on the 12-lead ECG does not take place on the short-term after ASD closure, despite clear RV geometrical remodeling within one-month post-closure reported by Veldtman et al. [19] Our results showed that QRS duration decreased at intermediate follow-up in both groups. While the presented slight change is clinically irrelevant, it may reflect ventricular electrical remodeling later after ASD closure. A recent study by Rucklova et al. [11] suggested that RV volume overload in ASDs is associated with prolonged repolarization. In their study it was shown that QTc-interval was significantly shorter at 6 months after ASD closure. In the present study we observed that the QTc-interval numerically shortens from the fourth week post-closure onwards, both in adults and children.

4.2. Mechanisms of VCG changes after percutaneous ASD closure

In the current study, we have approached the dynamics in the VCG by measuring two general vectorcardiographic properties, the VG and the spatial QRS-T angle. The VG reflects the integrated action potential duration (APD) inhomogeneity in the heart [5,22]. As such it is subject to cancellation and the magnitude and direction of the VG in a person expresses asymmetric inhomogeneity. Between individuals with normal hearts, the magnitude and direction of the VG varies considerably [23]. For this reason, individual trends in the VG are more informative than the overall VG value. In general, we may expect that any form of electrical remodeling in the heart is reflected in a change in the VG.

In an earlier study, the relation between the VG and RV pressure overload in patients with suspected pulmonary hypertension was shown [7]. VG changes were explained by different APD dynamics between subendocardial and epicardial myocytes as a result of RV pressure overload [24,25]. The hearts of ASD patients are characterized by RV volume overload rather than RV pressure overload. The RV volume overload in ASD patients results in APD prolongation in the RV epicardium [26]. Because successful ASD closure eliminates the volume overload [19], we expect normalization of the APD prolongation and therefore a change in the VG. In the current study, median VG magnitude was 63 [48–76] mV*ms in children before ASD closure, which is similar to the mean normal VG at 6.5 years of 69 mV*ms (2nd and 98th percentile: 24, 128) [27]. In adults, the VG magnitude before ASD closure was 66 [45–86], which is in the normal range for adults [23]. In children the VG magnitude showed an acute decrease, after which it increased again at intermediate follow-up. In adults the VG magnitude increased at late follow-up. A change in VG direction was most apparent in the azimuth becoming less negative at intermediate follow-up in both groups, while elevation decreased directly post-closure in the pediatric group but did not change during follow-up in the adult group. In our previous study on RV pressure overload [7], a preferential direction of the VG was found in which the VG changed with increasing pulmonary artery pressure. In the current study, however, we were not able to find a preferential direction in which the VG changed with decreasing RV volume overload due to successful ASD closure. The spatial QRS-T angle is the angle between the QRS axis and the T axis [5]. As such it can be considered a measure of concordance/discordance of the ECG: a small QRS-T angle represents a concordant ECG in which the QRS-complex and T-wave polarities assume the same values in most ECG-leads, whereas a large, obtuse, QRS-T angle represents a discordant ECG in which the QRS-complex and T-wave polarities assume opposite values in most ECG-leads. Generally, we may expect that changes in the QRS-complex or T-wave morphology always imply a change in the QRS and T axes, and, consequently, a change in the QRS-T angle. In many cases, an increase in the QRS-T angle is expected to represent a worsening condition. A larger spatial QRS-T angle has been linked to sudden cardiac death after acute coronary syndromes [28] and overall mortality in a general population [8]. Our study group included children of different ages with a median of 6 [4–11] years. Before closure of the ASD, median QRS-T angle was 52 [30–84]° in the children, which is larger than the mean normal QRS-T angle in children of 6.5 years of 20° but still within the normal range (2th and 98th percentile: 2, 85°) [27]. In the adult group the QRS-T angle was 42°, which is in the normal range for adults [23]. In both groups, the spatial QRS-T angle significantly decreased at late follow-up. This most likely reflects ventricular electrical remodeling occurring relatively late after ASD closure. Thus far, there are no data to suggest that a decrease in QRS-T angle also implies a lower risk of sudden death, arrhythmia or mortality in ASD patients.

4.3. Limitations

This study had several limitations. Not all patients had an ECG at all four time points and the study group consisted of a relatively small number of patients; hence, further studies with larger and more homogeneous patient groups and more complete ECG data are needed to confirm our findings. Also, this study only targeted ECG and VCG measurements and did not focus on accompanying hemodynamic and morphological data to correlate electrical and structural reverse remodeling. Finally, the ECG data in the current study consists of a mix of ECGs with sampling rates of 250, 500 and 1000 samples per second. However, because the studied QRS-T angle and the VG are computed from ECG integrals, it is unlikely that differences in sampling rate have consequences for the VCG findings in this study.

5. Conclusions

Successful percutaneous atrial septal defect closure was followed by a decrease in heart rate, P-wave amplitude, PQ duration, QRS duration and QTc interval in both children and adults. Changes mostly occurred directly after ASD closure except for QRS duration and QTc interval changes, which occurred later. Most of these electrocardiographic changes remained limited. The changes in the vectorcardiographic spatial QRS-T angle reflect increasing concordance of the electrocardiogram, which can be interpreted as partly normalization of the electrical properties of the heart. The ventricular gradient showed changes which can be seen as a result of action potential duration dynamics after atrial septal defect closure.

Acknowledgements

V.P. Kamphuis is financially supported by a grant from the Dutch Heart Foundation (Grant Number 2013T091). The authors thank C. ter Haar for her technical support. Also, the authors thank D. Raad for contributing to the LUMC database.

Disclosures

R.J. de Winter: Academic Medical Center received unrestricted institutional educational research grant from Abbott Vascular BV. All other authors report no relationships that could be construed as a conflict of interest.

Appendix A

Appendix Table 1
Subgroup analysis of adult patients with and without paroxysmal atrial fibrillation (n = 14 vs. n = 61).

	Baseline	Acute	*P*-value	Intermediate	*P*-value	Late	*P*-value
	Max −14 w	+1–7 d	Baseline-acute	+4–14 w	Baseline-intermediate	+6–18 m	Baseline-late
ECG results							
Adults with paroxysmal atrial fibrillation							
Heart rate, bpm	65 [61–75]	66 [61–73]	0.29	63 [56–74]	0.12	69 [49–74]	0.26
P-wave amplitude in lead II, mV	0.14 [0.08–0.17]	0.10 [0.07–0.12]	0.004	0.11 [0.07–0.16]	0.39	0.15 [0.10–0.17]	0.61
P-wave duration, ms	118 [109–133]	126 [111−133]	0.18	123 [101–135]	0.44	122 [106–144]	1.00

(continued on next page)

Appendix Table 1 (*continued*)

	Baseline	Acute	*P*-value	Intermediate	*P*-value	Late	*P*-value
	Max −14 w	+1–7 d	Baseline-acute	+4–14 w	Baseline-intermediate	+6–18 m	Baseline-late
PQ duration, ms	178 [162–195]	168 [157–204]	0.81	172 [156–194]	0.11	164 [152–184]	0.17
QRS duration, ms	109 [102–117]	113 [98–119]	0.53	108 [102–114]	0.04	101 [92–111]	0.02
QTc interval, ms	440 [424–460]	439 [415–451]	0.23	417 [409–469]	0.21	428 [409–438]	0.04
Adults without paroxysmal atrial fibrillation							
Heart rate, bpm	75 [61–84]	67 [58–78]	<0.001	65 [59–77]	0.04	65 [57–75	<0.001
P-wave amplitude in lead II, mV	0.15 [0.10–0.16]	0.11 [0.08–0.15]	<0.001	0.13 [0.11–0.15]	0.17	0.14 [0.12–0.17]	0.72
P-wave duration, ms	114 [105–124]	113 [104–124]	0.30	112 [102−122]	0.29	112 [104–122]	0.08
PQ duration, ms	160 [146–177]	162 [146–183]	0.64	150 [142–172]	0.05	156 [141–172]	0.02
QRS duration, ms	106 [93–116]	107 [93–116]	0.62	98 [89–111]	0.02	102 [92–109]	<0.001
QTc interval, ms	431 [413–451]	431 [416–447]	0.37	418 [407–440]	0.01	416 [403–431]	0.001
Adults whole group							
Heart rate, bpm	72 [61–81]	67 [59–78]	<0.001	65 [58–76]	0.01	65 [56–74]	<0.001
P-wave amplitude in lead II, mV	0.15 [0.10–0.16]	0.11 [0.08–0.14]	<0.001	0.13 [0.10–0.16]	0.07	0.14 [0.11–0.17]	0.63
P-wave duration, ms	115 [106–125]	114 [104–126]	0.63	112 [102−123]	0.20	113 [104–124]	0.11
PQ duration, ms	163 [150–184]	162 [148–185]	0.62	157 [144–172]	0.01	106 [94–116]	0.009
QRS duration, ms	106 [94–116]	108 [94–118]	0.46	101 [91–112]	0.004	102 [92–109]	<0.001
QTc interval, ms	432 [414–451]	433 [416–449]	0.20	418 [407–441]	0.005	417 [404–435]	<0.001
VCG results							
Adults with paroxysmal atrial fibrillation							
Spatial QRS-T angle, °	65 [54–112]	70 [52–114]	0.59	45 [16–62]	0.04	41 [14–59]	0.16
VG magnitude, mV·ms	52 [29–78]	48 [27–66]	0.16	74 [44–92]	0.02	71 [60–154]	0.09
VG azimuth, °	−16 [−33−3]	−18 [−28–22]	0.42	−2 [−17–12]	0.01	−18 [−27–0.5]	0.26
VG elevation, °	36 [29–55]	33 [24–42]	0.13	28 [23–37]	0.05	31 [23–41]	1.00
Adults without paroxysmal atrial fibrillation							
Spatial QRS-T angle, °	34 [20–77]	31 [21–56]	0.22	28 [18–42]	0.03	36 [22–48]	0.01
VG magnitude, mV·ms	68 [46–87]	68 [40–91]	0.69	75 [50–96]	0.53	70 [56–85]	0.004
VG azimuth, °	−12 [−25 to −2]	−15 [−25 to −3]	0.34	−9 [−18–0.5]	0.004	−7 [−23−2]	0.11
VG elevation, °	40 [33–47]	37 [29–41]	<0.001	37 [34–44]	0.39	39 [32–45]	0.68
Adults whole group							
Spatial QRS-T angle, °	42 [21–82]	38 [22–70]	0.79	30 [17–45]	0.39	36 [20–48]	0.001
VG magnitude, mV·ms	66 [45–86]	63 [37–89]	0.32	75 [50–94]	0.08	70 [56–89]	0.001
VG azimuth, °	−12 [−26–0]	−15 [−24 to −3]	0.70	−7 [−17–3]	<0.001	−8 [−24–1]	0.48
VG elevation, °	39 [32–47]	36 [29–41]	<0.001	37 [31–44]	0.07	38 [29–45]	0.65

Data are presented as median [25th–75th percentile].
d = days; w = weeks; m = months.

Appendix B. Supplementary data

Supplementary data to this article can be found online at https://doi.org/10.1016/j.ijcard.2019.02.020.

References

[1] J.B. Lindsey, L.D. Hillis, Clinical update: atrial septal defect in adults, Lancet 369 (2007) 1244–1246.

[2] H. Baumgartner, P. Bonhoeffer, N.M. De Groot, F. de Haan, J.E. Deanfield, N. Galie, M.A. Gatzoulis, C. Gohlke-Baerwolf, H. Kaemmerer, P. Kilner, F. Meijboom, B.J. Mulder, E. Oechslin, J.M. Oliver, A. Serraf, A. Szatmari, E. Thaulow, P.R. Vouhe, E. Walma, Task Force on the Management of Grown-up Congenital Heart Disease of the European Society of C, Association for European Paediatric C and Guidelines ESCCfP, ESC Guidelines for the management of grown-up congenital heart disease (new version 2010), Eur. Heart J. 31 (2010) 2915–2957.

[3] R.T. Grignani, K.M. Tolentino, D.D. Rajgor, S.C. Quek, Longitudinal evaluation of P-wave dispersion and P-wave maximum in children after transcatheter device closure of secundum atrial septal defect, Pediatr. Cardiol. 36 (2015) 1050–1056.

[4] O. Monfredi, M. Luckie, H. Mirjafari, T. Willard, H. Buckley, L. Griffiths, B. Clarke, V.S. Mahadevan, Percutaneous device closure of atrial septal defect results in very early and sustained changes of right and left heart function, Int. J. Cardiol. 167 (2013) 1578–1584.

[5] S. Man, A.C. Maan, M.J. Schalij, C.A. Swenne, Vectorcardiographic diagnostic & prognostic information derived from the 12-lead electrocardiogram: historical review and clinical perspective, J. Electrocardiol. 48 (2015) 463–475.

[6] J.A. Kors, G. van Herpen, A.C. Sittig, J.H. van Bemmel, Reconstruction of the Frank vectorcardiogram from standard electrocardiographic leads: diagnostic comparison of different methods, Eur. Heart J. 11 (1990) 1083–1092.

[7] V.P. Kamphuis, M.L. Haeck, G.S. Wagner, A.C. Maan, C. Maynard, V. Delgado, H.W. Vliegen, C.A. Swenne, Electrocardiographic detection of right ventricular pressure overload in patients with suspected pulmonary hypertension, J. Electrocardiol. 47 (2014) 175–182.

[8] J.W. Waks, C.M. Sitlani, E.Z. Soliman, M. Kabir, E. Ghafoori, M.L. Biggs, C.A. Henrikson, N. Sotoodehnia, T. Biering-Sorensen, S.K. Agarwal, D.S. Siscovick, W.S. Post, S.D. Solomon, A.E. Buxton, M.E. Josephson, L.G. Tereshchenko, Global electric heterogeneity risk score for prediction of sudden cardiac death in the general population: the Atherosclerosis Risk in Communities (ARIC) and Cardiovascular Health (CHS) studies, Circulation 133 (2016) 2222–2234.

[9] F. Fang, X.X. Luo, Q.S. Lin, J.S. Kwong, Y.C. Zhang, X. Jiang, C.M. Yu, Y.Y. Lam, Characterization of mid-term atrial geometrical and electrical remodeling following device closure of atrial septal defects in adults, Int. J. Cardiol. 168 (2013) 467–471.

[10] M.G. Kaya, A. Baykan, A. Dogan, T. Inanc, O. Gunebakmaz, O. Dogdu, K. Uzum, N.K. Eryol, N. Narin, Intermediate-term effects of transcatheter secundum atrial septal defect closure on cardiac remodeling in children and adults, Pediatr. Cardiol. 31 (2010) 474–482.

[11] K. Rucklova, K. Koubsky, V. Tomek, P. Kubus, J. Janousek, Prolonged repolarization in atrial septal defect: an example of mechanoelectrical feedback due to right ventricular volume overload, Heart Rhythm. 13 (2016) 1303–1308.

[12] U. Thilen, J. Carlson, P.G. Platonov, S.B. Olsson, Atrial myocardial pathoelectrophysiology in adults with a secundum atrial septal defect is unaffected by closure of the defect. A study using high resolution signal-averaged orthogonal P-wave technique, Int. J. Cardiol. 132 (2009) 364–368.

[13] J.A. Kors, G. van Herpen, Methodology of QT-interval measurement in the modular ECG analysis system (MEANS), Ann. Noninvasive Electrocardiol. 14 (Suppl. 1) (2009) S48–S53.

[14] J.H. van Bemmel, J.A. Kors, G. van Herpen, Methodology of the modular ECG analysis system MEANS, Methods Inf. Med. 29 (1990) 346–353.

[15] J.L. Willems, P. Arnaud, J.H. van Bemmel, P.J. Bourdillon, R. Degani, B. Denis, I. Graham, F.M. Harms, P.W. Macfarlane, G. Mazzocca, et al., A reference data base for multilead electrocardiographic computer measurement programs, J. Am. Coll. Cardiol. 10 (1987) 1313–1321.

[16] Report of committee on electrocardiography, American Heart Association, Recommendations for standardization of leads and of specifications for instruments in electrocardiography and vectorcardiography, Circulation 35 (1967) 583–602.

[17] J.B. Morton, P. Sanders, J.K. Vohra, P.B. Sparks, J.G. Morgan, S.J. Spence, L.E. Grigg, J.M. Kalman, Effect of chronic right atrial stretch on atrial electrical remodeling in patients with an atrial septal defect, Circulation 107 (2003) 1775–1782.

[18] J. Heller, A.A. Hagege, B. Besse, M. Desnos, F.N. Marie, C. Guerot, "Crochetage" (notch) on R wave in inferior limb leads: a new independent electrocardiographic sign of atrial septal defect, J. Am. Coll. Cardiol. 27 (1996) 877–882.

[19] G.R. Veldtman, V. Razack, S. Siu, H. El-Hajj, F. Walker, G.D. Webb, L.N. Benson, P.R. McLaughlin, Right ventricular form and function after percutaneous atrial septal defect device closure, J. Am. Coll. Cardiol. 37 (2001) 2108–2113.

[20] G.J. Crystal, M.R. Salem, The Bainbridge and the "reverse" Bainbridge reflexes: history, physiology, and clinical relevance, Anesth. Analg. 114 (2012) 520–532.

[21] E.A. MacDonald, M.R. Stoyek, R.A. Rose, T.A. Quinn, Intrinsic regulation of sinoatrial node function and the zebrafish as a model of stretch effects on pacemaking, Prog. Biophys. Mol. Biol. 130 (2017) 198–211.
[22] H.H. Draisma, M.J. Schalij, E.E. van der Wall, C.A. Swenne, Elucidation of the spatial ventricular gradient and its link with dispersion of repolarization, Heart Rhythm. 3 (2006) 1092–1099.
[23] R.W. Scherptong, I.R. Henkens, S.C. Man, S. Le Cessie, H.W. Vliegen, H.H. Draisma, A.C. Maan, M.J. Schalij, C.A. Swenne, Normal limits of the spatial QRS-T angle and ventricular gradient in 12-lead electrocardiograms of young adults: dependence on sex and heart rate, J. Electrocardiol. 41 (2008) 648–655.
[24] C. Shi, X. Wang, F. Dong, Y. Wang, J. Hui, Z. Lin, J. Yang, Y. Xu, Temporal alterations and cellular mechanisms of transmural repolarization during progression of mouse cardiac hypertrophy and failure, Acta Physiol (Oxf) 208 (2013) 95–110.
[25] Y. Tanaka, B. Takase, T. Yao, M. Ishihara, Right ventricular electrical remodeling and arrhythmogenic substrate in rat pulmonary hypertension, Am. J. Respir. Cell Mol. Biol. 49 (2013) 426–436.
[26] N. Izumida, Y. Asano, H. Wakimoto, M. Nishiyama, S. Doi, S. Tsuchiya, J. Hosaki, S. Kawano, T. Sawanobori, M. Hiraoka, Analysis of T wave changes by activation recovery interval in patients with atrial septal defect, Int. J. Cardiol. 74 (2000) 115–124.
[27] V.P. Kamphuis, N.A. Blom, E.W. van Zwet, S. Man, A.D.J. Ten Harkel, A.C. Maan, C.A. Swenne, Normal values of the ventricular gradient and QRS-T angle, derived from the pediatric electrocardiogram, J. Electrocardiol. 51 (2018) 490–495.
[28] M. Lingman, M. Hartford, T. Karlsson, J. Herlitz, A. Rubulis, K. Caidahl, L. Bergfeldt, Value of the QRS-T area angle in improving the prediction of sudden cardiac death after acute coronary syndromes, Int. J. Cardiol. 218 (2016) 1–11.